

Enhanced Electrocatalytic Hydrogen Evolution by Molybdenum Disulfide Nanodots Anchored on MXene under Alkaline Conditions

Xiaoyu Wang^{1‡}, Wenbin You^{2‡}, Liting Yang², Guanyu Chen², Zhengchen Wu², Chang Zhang², Qianjin Chen^{1*}, and Renchao Che^{2,3*}

Experimental section

Materials and Chemicals. Ti_3AlC_2 powders were purchased from Laizhou Kai Kai Ceramic Materials Company. Ammonium molybdate ($(\text{NH}_4)_6\text{Mo}_7\text{O}_{24}\cdot 4\text{H}_2\text{O}$), dopamine hydrochloride ($\text{C}_8\text{H}_{12}\text{ClNO}_2$), sublimed sulfur (S), and potassium hydroxide (KOH) were purchased from Aladdin Reagent Limited Company. Ethanol, ammonia water, LiF, and HCl were purchased from Sinopharm Chemical Limited Reagent Company. All the reagents used in this work were analytically pure without further purification. Deionized water was used in all experiments treated by the Milli-Q system (Millipore, Bedford, MA).

Synthesis of $\text{Ti}_3\text{C}_2\text{T}_x$ MXene. Firstly, 1 g Ti_3AlC_2 MAX was etched in 20 mL HCl (9 M) solution with 1.6 g LiF for 24 h. Then, the etched mixture was diluted with 140 mL of deionized water and centrifuged at 3,500 rpm for 5 min to discard the acid solution. After repeating several times, the dark-green supernatant was collected and discarded the unetched Ti_3AlC_2 . Finally, a single-layer or few-layer $\text{Ti}_3\text{C}_2\text{T}_x$ MXene precipitate was collected by centrifugation at 10000 rpm for half an hour, and freeze-dried overnight²⁸.

Synthesis of MXene/NF, MoO_3 /NF, MoO_3 /MXene/NF. The Mo-PDA/MXene/NF precursor was prepared firstly in the pretreated nickel foam. Typically, 20 mg MXene and 50 mg ammonium molybdate tetrahydrate were dissolved in 10 mL of deionized water, and NF was placed in the above solution saturated with nitrogen protection for 30 min. Then 50 mg dopamine hydrochloride was dissolved in 20 mL of ethanol. Next, the two solutions were mixed, and subsequently, 0.1 mL of ammonium hydroxide was quickly added to the mixture solution. After stirring for 5 min, Mo-PDA/MXene/NF was obtained by washing the product with ethanol. Mo-PDA/NF was prepared by the same procedure without adding $\text{Ti}_3\text{C}_2\text{T}_x$ MXene, while PDA/MXene/NF was obtained by the same method without adding ammonium

molybdate tetrahydrate. All the samples were lyophilized at $-80\text{ }^{\circ}\text{C}$ for further use. Finally, MXene/NF, MoO_3/NF , $\text{MoO}_3/\text{MXene}/\text{NF}$ were obtained after annealing PDA/MXene/NF, Mo-PDA/NF, and Mo-PDA/ $\text{Ti}_3\text{C}_2\text{T}_x/\text{NF}$ at $650\text{ }^{\circ}\text{C}$ for 3 h with a heating rate of $2\text{ }^{\circ}\text{C min}^{-1}$ under N_2 atmosphere.

Synthesis of MoS_2/NF , $\text{MoS}_2/\text{MXene}/\text{NF}$. The as-prepared MoO_3/NF and $\text{MoO}_3/\text{MXene}/\text{NF}$ were sulfurized in a tube furnace system for 2 h with argon carried sublimed sulfur as the sulfur source (the gas flowing rate at 20 sccm). The MoO_3 in MoO_3/NF and $\text{MoO}_3/\text{MXene}/\text{NF}$ transformed into MoS_2 under sulfurization temperatures from 500 to $800\text{ }^{\circ}\text{C}$.

Material characterization. The crystal phases of samples were characterized by powder X-ray diffraction (XRD, Bruker D8 ADVANCE, at 40 kV and 40 mA). Field emission scanning electron microscope (FESEM, Hitachi S-4800, accelerating voltage 5 kV) and transmission electron microscope (TEM, JEOL JEM-2100F, accelerating voltage 200 kV) were used for the morphology research. In addition, TEM was also used for element distribution mapping. The elemental chemical valence was analyzed by X-ray photoelectron spectroscopy (XPS, ESCALAB210).

Electrochemical tests. The CHI760D workstation was used to carry out electrochemical tests *via* a traditional three-electrode method, in which 1 M KOH solution was employed as the electrolyte with N_2 gas flowing continuously bubbled. The three electrodes are the carbon rod as the counter electrode, the saturated calomel electrode (SCE) as the reference electrode, and the prepared $\text{MoS}_2/\text{MXene}/\text{NF}$ as the working electrode, respectively. Linear sweep voltammetry (LSV) is measured at a sweep rate of $5\text{ mV}\cdot\text{s}^{-1}$ after cyclic voltammetry (CV) cycles. Electrochemical impedance spectroscopy (EIS) is tested in the 10^6 -0.01 Hz frequency range. To evaluate the electrochemical active area (ECSA) of the $\text{MoS}_2/\text{MXene}/\text{NF}$, the electric double-layer capacitance (C_{dl}) is characterized by CV with 20 - $100\text{ mV}\cdot\text{s}^{-1}$ sweep speeds. The stability of the working electrode is evaluated by comparing the changes in the LSV polarization curves before and after 2000 CV cycles. All electrode potentials mentioned during the electrochemical tests were converted and related to the reversible hydrogen electrode (RHE) by the Nernst equation: $E(\text{RHE})=E(\text{SCE}) + 0.2412 + 0.0591\times\text{pH}$ (V). Meanwhile, the LSV test result was calibrated by ohmic (IR) losses based on EIS measurements.

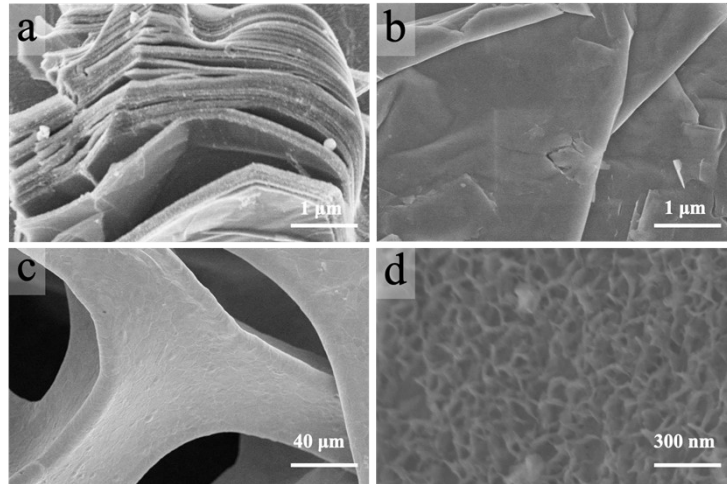


Figure S1. SEM images of (a) MAX, (b) Ti₃C₂T_x MXene (c) NF at low magnification, and (d) Mo-PDA/MXene/NF.

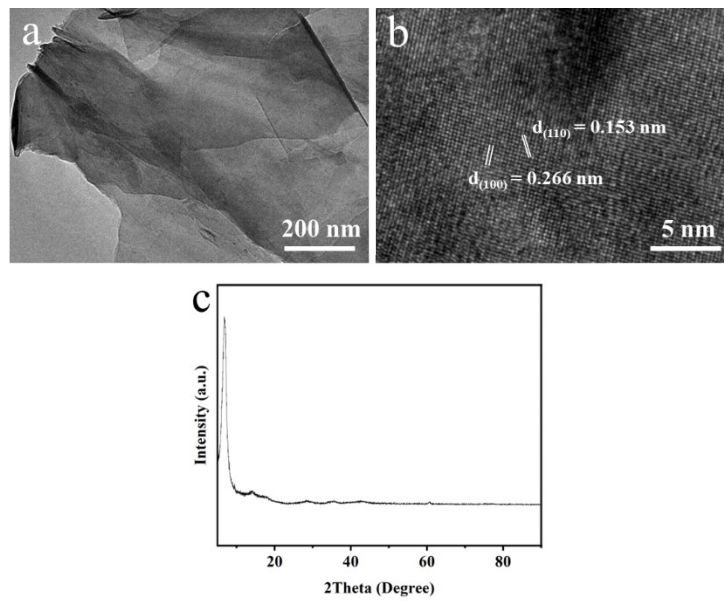


Figure S2. (a) TEM image, (b) HRTEM image, and XRD pattern of Ti₃C₂T_x.

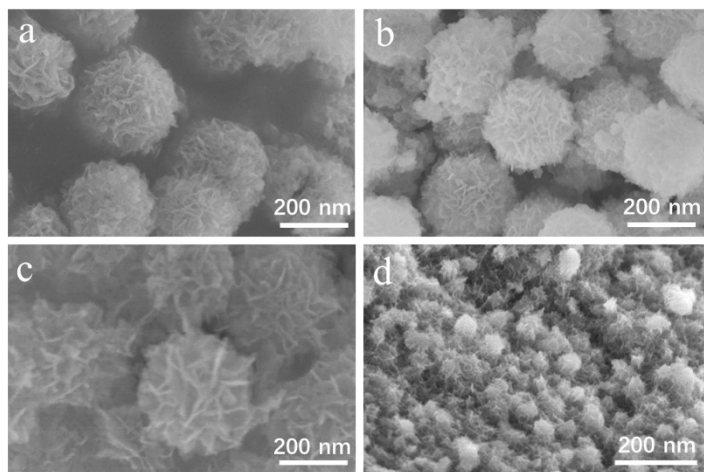


Figure S3. SEM images of (a) Mo-PDA/NF, (b) MoO₃/NF, (c) MoS₂/NF, and (d) MoS₂/NF after electrochemical tests.

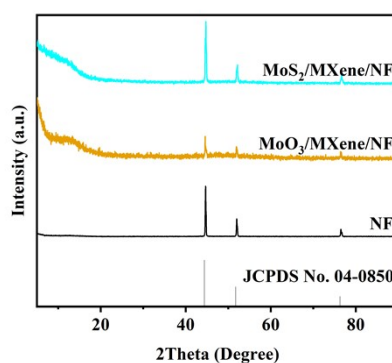


Figure S4. XRD patterns NF, MoO₃/MXene/NF, and MoS₂/MXene/NF.

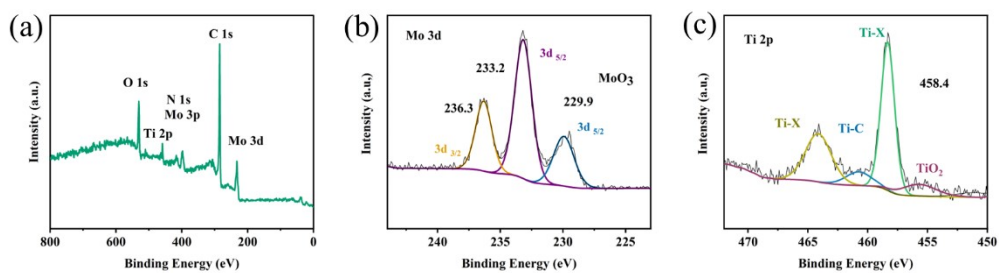


Figure S5. (a) full spectrum of MoO₃/MXene shaved from MoO₃/MXene/NF. Corresponding high-resolution XPS spectra of (b) Mo 3d and (c) Ti 2p.

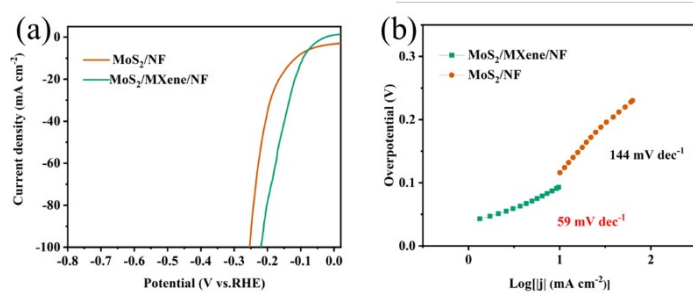


Figure S6. (a) Polarization curves and (b) corresponding Tafel plots of MoS₂/MXene/NF and NF in 1 M KOH.

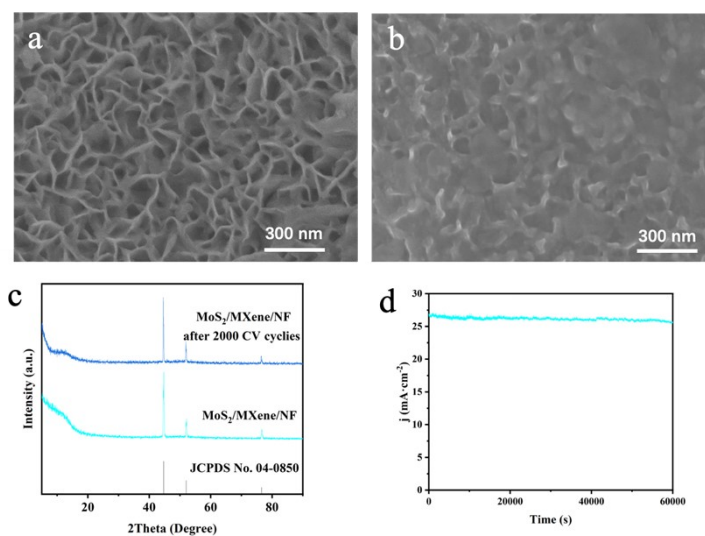


Figure S7. SEM images of MoS₂/MXene/NF (a) before and (b) after 2000 cyclic potential scans. (c) the corresponding XRD patterns (d) Chronoamperometric curve of MoS₂/MXene/NF.

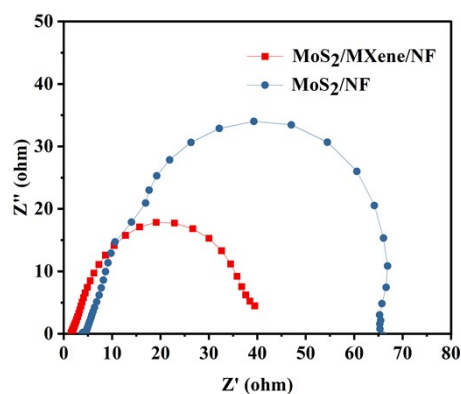


Figure S8. Nyquist plots of the MoS₂/MXene/NF and NF.

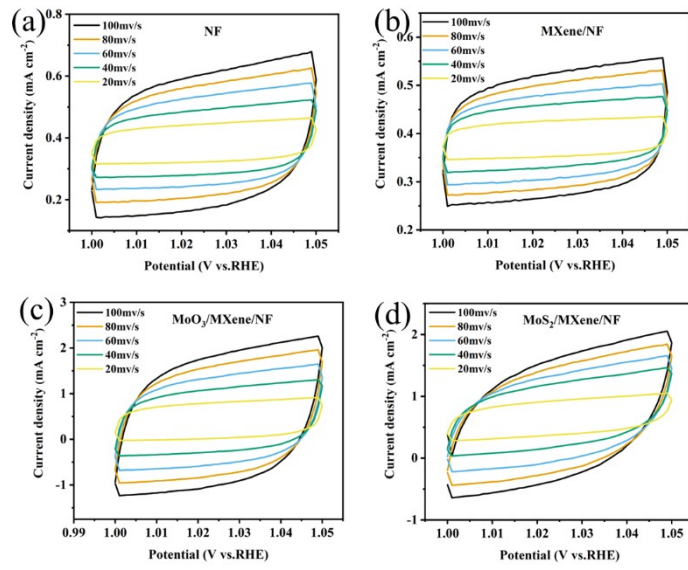


Figure S9. CV curves at different scan rates of (a) NF, (b) Mxene/NF, (c) MoO₃/MXene/NF, and (d) MoS₂/MXene/NF.

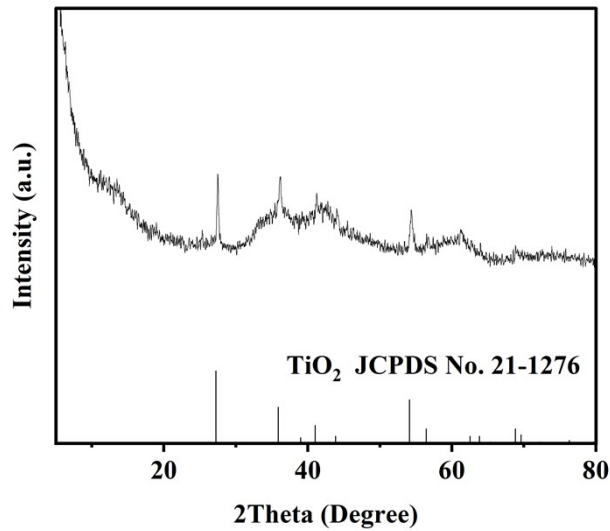


Figure S10. XRD pattern of MoS₂/MXene shaved from MoS₂/MXene/NF after sulfurization at 800 °C.

Table S1 The comparison of the HER performance of the samples

Catalysts	Overpotential (mV) at 10 mA cm ⁻²	Tafel slope (mV dec ⁻¹)	Ref.
Mxene	169	97	1
MoS _{2-x} / FTO	310	84	2
MoS _{2+x} / Ni	210	84	2
MoS ₂ /Ni	184	87	3
Co-MoS ₂	200	79	4
Fe-MoS ₂	203	181	4
3D-MoS ₂ /Mo	163	158	5
MoS ₂ /Ni ₃ S ₂ /NF	199	83	6
Co-MoNiS/NF	166	85	7
Ni ₂ P/MoS ₂ /N:RGO	149	62	8
Mo-N/C@MoS ₂	117	64.3	9
2D-MoS ₂ /Ni(OH) ₂	185	73	10
Mo ₂ N-Mo ₂ C/HGr-3	154	68	11
MoS ₂ @C	155	99	12
Pt/C	64	39	13
MoS ₂ /MXene/NF	94	59	This work

References

- 1.C. G. Morales-Guio, L. Liardet, M. T. Mayer, S. D. Tilley, M. Graetzel and X. Hu, *Angewandte Chemie- International Edition*, 2015, 54, 664-667.
- 2.D. Voiry, R. Fullon, J. Yang, C. d. C. Castro e Silva, R. Koppera, I. Bozkurt, D. Kaplan, M. J. Lagos, P. E. Batson, G. Gupta, A. D. Mohite, L. Dong, D. Er, V. B. Shenoy, T. Asefa and M. Chhowalla, *Nature Materials*, 2016, 15, 1003-1009.
3. B. Zhang, J. Liu, J. Wang, Y. Ruan, X. Ji, K. Xu, C. Chen, H. Wan, L. Miao and J. Jiang, *Nano Energy*, 2017, 37, 74-80.
4. J. Lin, P. Wang, H. Wang, C. Li, X. Si, J. Qi, J. Cao, Z. Zhong, W. Fei and J. Feng, *Advanced Science*, 2019, 6.
5. Y. Yang, H. Yao, Z. Yu, S. M. Islam, H. He, M. Yuan, Y. Yue, K. Xu, W. Hao, G. Sun, H. Li, S. Ma, P. Zapoland M. G. Kanatzidis, *Journal of the American Chemical Society*, 2019, 141, 10417-1043

6. G. Zhao, P. Li, K. Rui, Y. Chen, S. X. Dou and W. Sun, *Chemistry-a European Journal*, 2018, 24, 11158-11165.
7. J. Liu, Y. Liu, D. Xu, Y. Zhu, W. Peng, Y. Li, F. Zhang and X. Fan, *Applied Catalysis B-Environmental*, 2019, 241, 89-94.
8. Kim, M.; Anjum, M. A. R.; Lee, M.; Lee, B. J.; Lee, J. S., Activating MoS₂ Basal Plane with Ni₂P Nanoparticles for Pt-Like Hydrogen Evolution Reaction in Acidic Media. *Advanced Functional Materials* **2019**, 29 (10).
9. Li, Y.; Dong, Z.; Jiao, L., Multifunctional Transition Metal-Based Phosphides in Energy-Related Electrocatalysis. *Advanced Energy Materials* **2020**, 10 (11).
10. Zhu, Z.; Yin, H.; He, C.-T.; Al-Mamun, M.; Liu, P.; Jiang, L.; Zhao, Y.; Wang, Y.; Yang, H.-G.; Tang, Z.; Wang, D.; Chen, X.-M.; Zhao, H., Ultrathin Transition Metal Dichalcogenide/3d Metal Hydroxide Hybridized Nanosheets to Enhance Hydrogen Evolution Activity. *Advanced Materials* **2018**, 30 (28).
11. Yan, H.; Xie, Y.; Jiao, Y.; Wu, A.; Tian, C.; Zhang, X.; Wang, L.; Fu, H., Holey Reduced Graphene Oxide Coupled with an Mo₂N-Mo₂C Heterojunction for Efficient Hydrogen Evolution. *Advanced Materials* **2018**, 30 (2).
12. Xu, Q.; Liu, Y.; Jiang, H.; Hu, Y.; Liu, H.; Li, C., Unsaturated Sulfur Edge Engineering of Strongly Coupled MoS₂ Nanosheet-Carbon Macroporous Hybrid Catalyst for Enhanced Hydrogen Generation. *Advanced Energy Materials* **2019**, 9 (2).
13. Yang, Y.; Yao, H.; Yu, Z.; Islam, S. M.; He, H.; Yuan, M.; Yue, Y.; Xu, K.; Hao, W.; Sun, G.; Li, H.; Ma, S.; Zapol, P.; Kanatzidis, M. G., Hierarchical Nanoassembly of MoS₂/Co₉S₈/Ni₃S₂/Ni as a Highly Efficient Electrocatalyst for Overall Water Splitting in a Wide pH Range. *Journal of the American Chemical Society* **2019**, 141 (26), 10417-10430.